Supporting Information for Interfacial Electron Transfer and Ion Solvation in the Solid Electrolyte Interphase

Jeongmin Kim,[†] Brett M. Savoie,[‡] and Thomas F. Miller III[*,†]

†*Division of Chemistry and Chemical Engineering, California Institute of Technology, Pasadena, California, USA*

‡*School of Chemical Engineering, Purdue University, West Lafayette, Indiana, USA*

E-mail: tfm@caltech.edu

S1 Mean electric potential

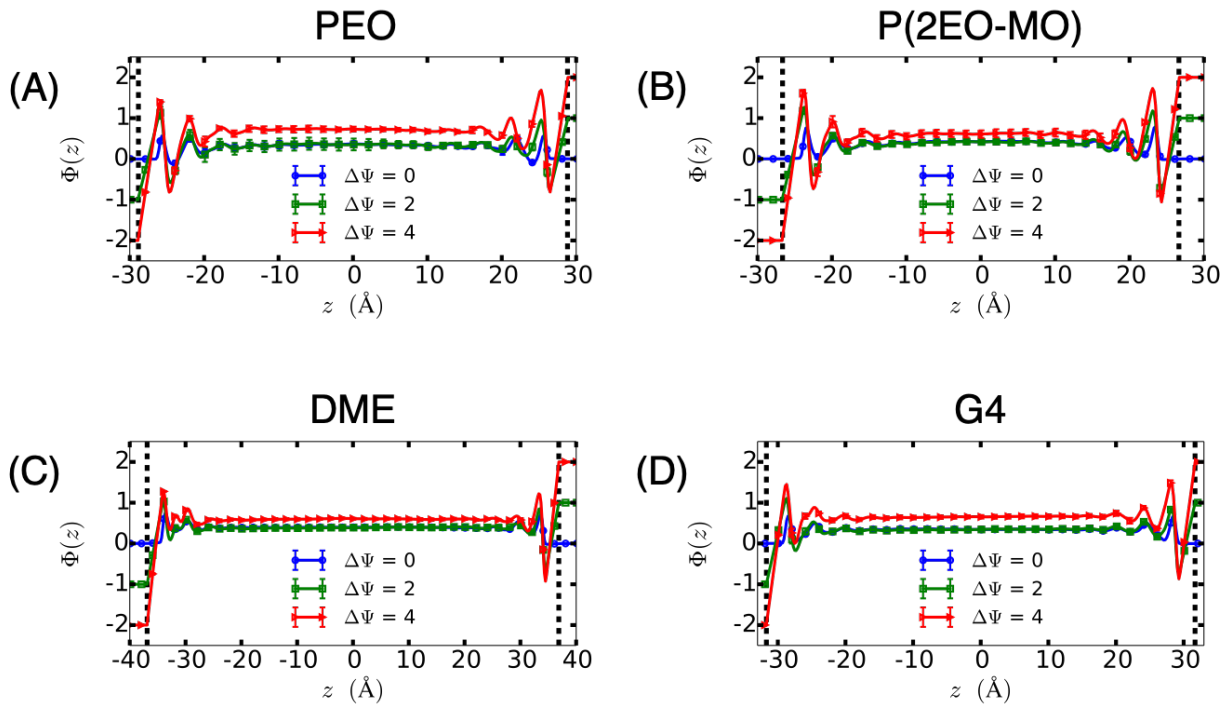

Figure S1: Mean electric potential across the simulation cell for the various electrolytes and bias potentials. In all panels, the black vertical line indicates the location of the electrolyte-exposed layer of the anode.

Fig. S1 shows mean electric potential, $\Phi(z)$ calculated, solving Poisson equation numerically across the simulation cell.[1,2]

$$\frac{d^2\Phi(z)}{dz^2} = -\frac{\rho(z)}{\epsilon_0}, \tag{1}$$

where $\rho(z)$ is the mean charge density averaged over a xy plane, and ϵ_0 is vacuum permittivity. In all considered electrolytes, $\Phi(z)$ oscillates at the electrode interface due to the electrical double layer. After the screening from the interfacial ions, $\Phi(z)$ reaches the plateau.

S2 Spatially-resolved lithium-ion solvation motif at the anode interface

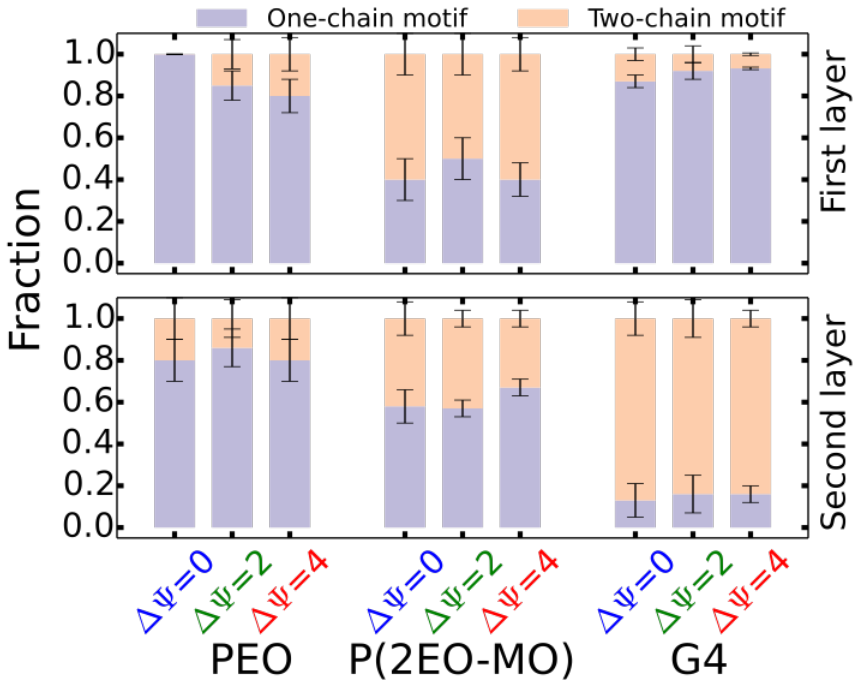

Figure S2: Spatially-resolved lithium-ion solvation motif at the anode interface. A top panel is for the first layer of interfacial lithium-ions, and a bottom panel is for the second layer of interfacial lithium-ions. For PEO and P(2EO-MO), the first layer is a region of $d \in (2, 7)$, and the second layer is a region of $d \in [7, 11)$. For G4, the first layer is a region of $d \in (2, 4.5)$, and the second layer is a region of $d \in [4.5, 7)$. The distance (d) is from the anode.

S3 Outer-sphere ET at the anode interface

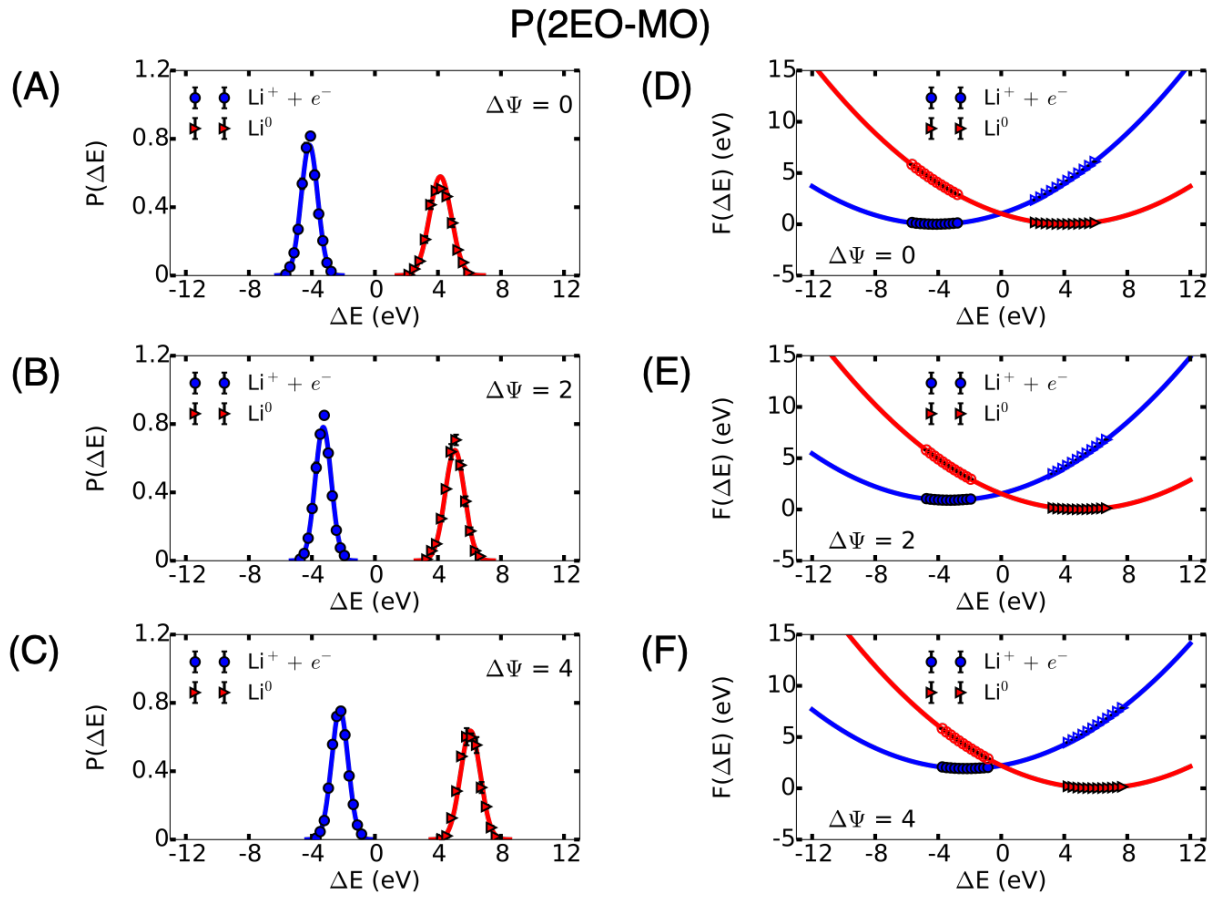

Figure S3: Lithium electroreduction in P(2EO-MO) at the anode interface. (A, B, and C) Probability distributions $P(\Delta E)$ of the vertical energy gap ΔE, and (D, E, and F) their associated free energy curves for both the Li^+ and Li^0 in P(2EO-MO). Results are shown for various bias potentials. Solid lines in (D, E, and F) are parabolic curves using linear-response assumptions.

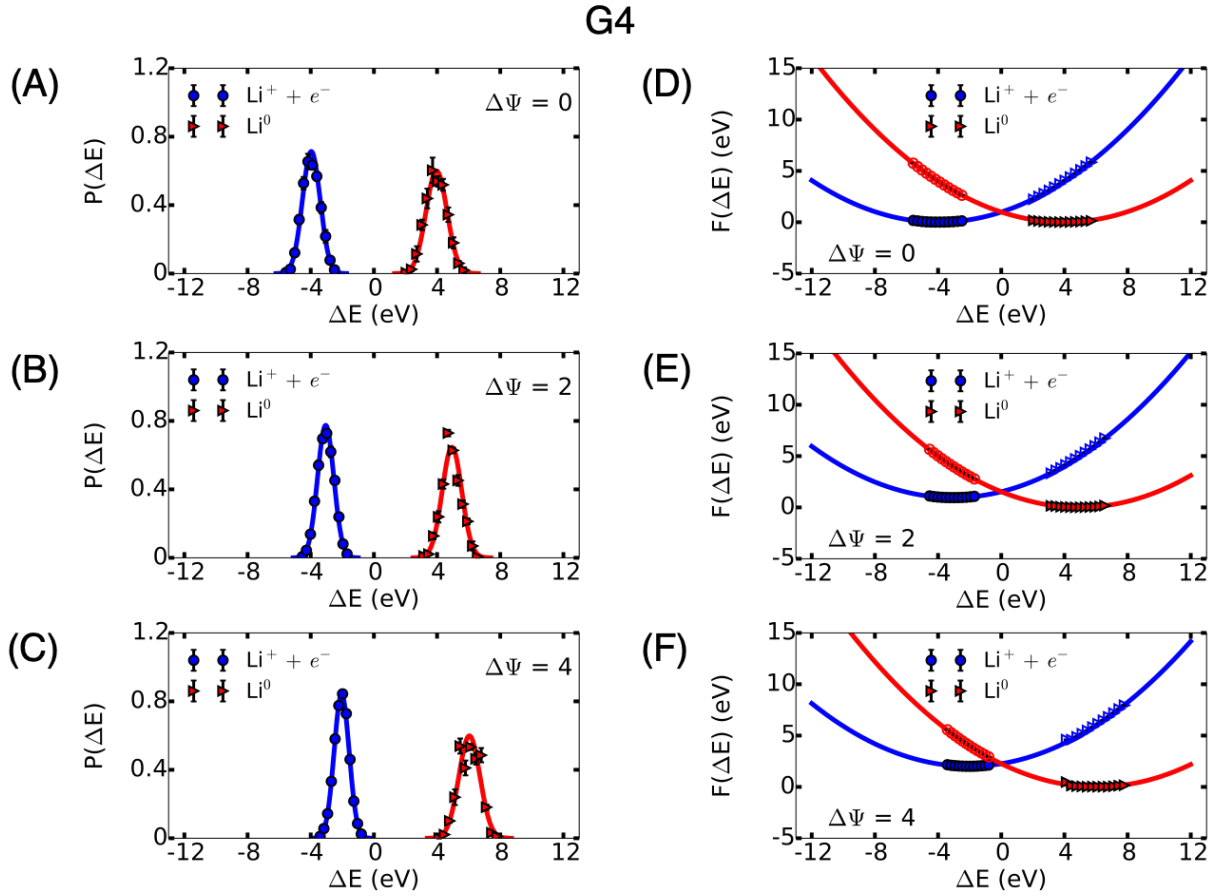

Figure S4: Lithium electroreduction in G4 at the anode interface. (A, B, and C) Probability distributions $P(\Delta E)$ of the vertical energy gap ΔE, and (D, E, and F) their associated free energy curves for both the Li^+ and Li^0 in G4. Results are shown for various bias potentials. Solid lines in (D, E, and F) are parabolic curves using linear-response assumptions.

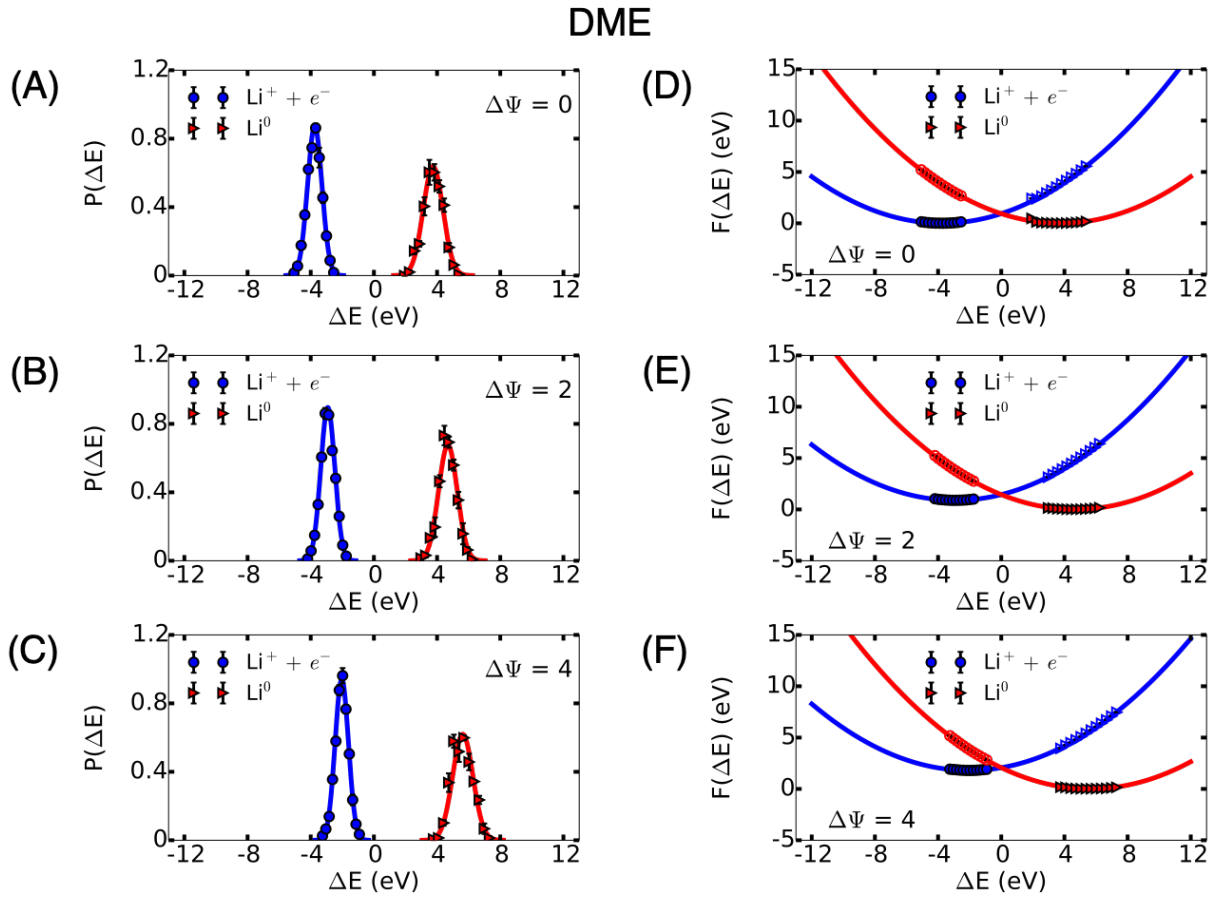

Figure S5: Lithium electroreduction in DME at the anode interface. (A, B, and C) Probability distributions $P(\Delta E)$ of the vertical energy gap ΔE, and (D, E, and F) their associated free energy curves for both the Li^+ and Li^0 in DME. Results are shown for various bias potentials. Solid lines in (D, E, and F) are parabolic curves using linear-response assumptions.

References

(1) Reed, S. K.; Madden, P. A.; Papadopoulos, A. Electrochemical charge transfer at a metallic electrode: a simulation study. *The Journal of Chemical Physics* **2008**, *128*, 124701.

(2) Giordano, N. *Computational Physics*; Prentice Hall, 1997.